Neutron scattering study of acoustic phonon softening in $BiVO_4$

Izumi Tomeno,[1,*] Naomi Sato,[1] Yoshinosuke Sato,[1] Kunihiko Oka,[2] and Yorihiko Tsunoda[3]
[1]*Faculty of Education and Human Studies, Akita University, Akita 010-8502, Japan*
[2]*Nanoelectronics Research Institute, National Institute of Advanced Industrial Science and Technology, Tsukuba, Ibaraki 305-8568, Japan*
[3]*Department of Applied Physics, School of Science and Engineering, Waseda University, Shinjuku, Tokyo 169-8555, Japan*
(Received 21 October 2010; revised manuscript received 8 May 2011; published 12 July 2011)

Inelastic neutron scattering has been used to study the transverse acoustic (TA) phonon propagating on the (0,0,1) plane polarized on this plane in $BiVO_4$ above the ferroelastic phase transition at $T_c = 528$ K. The energies of the TA phonon dispersion curve along $[0.7\xi,\xi,0]$ are slightly lower than those along $[\xi,\xi,0]$, indicating that the acoustic symmetry direction deviates from the high-symmetry $[\xi,\xi,0]$ direction. The $[0.7\xi,\xi,0]$ TA branch softens in a limited range $\xi \lesssim 0.2$ as the temperature approaches T_c from above. The gradual decrease in the initial slope of the $[0.7\xi,\xi,0]$ TA branch is quite different from the complete softening of the TA mode reported from Brillouin scattering measurements. A temperature-dependent central peak is associated with the $[0.7\xi,\xi,0]$ TA mode. Furthermore, an elastic diffuse streak along $[1,\bar{1},0]$ exists up to 878 K. These precursor effects are discussed in connection with the TA phonon softening.

DOI: 10.1103/PhysRevB.84.014302 PACS number(s): 63.20.−e

I. INTRODUCTION

Bismuth vanadate $BiVO_4$ is of particular interest for both fundamental and practical reasons because it exhibits ferroelasticity,[1] oxygen ion conductivity,[2] and photocatalytic activity.[3] The compound $BiVO_4$ undergoes a second-order ferroelastic phase transition at $T_c = 528$ K.[1,4] The high-temperature paraelastic phase has a body-centered tetragonal scheelite structure with a centrosymmetric space group $I4_1/a$ (C_{4h}^6).[5] The primitive cell consists of two formula units, as shown in Fig. 1. The Bi and V sites have S_4 point symmetry, whereas the O sites have the lowest site symmetry C_1. The projection of the crystal structure on the (0,0,1) plane demonstrates that the isolated VO_4 tetrahedra are rotated about the [0, 0,1] axis. The low-temperature ferroelastic phase has a monoclinic distorted scheelite structure with $I2/a$ (C_{2h}^6).

Considerable effort has been devoted to studying phonon anomalies associated with the ferroelastic phase transition in $BiVO_4$. Brillouin scattering studies[6,7] revealed a complete softening of transverse acoustic (TA) modes polarized on the (0,0,1) plane at T_c. Raman scattering[8,9] also showed a slight softening of transverse optic (TO) modes with B_g symmetry toward T_c. The simultaneous softening in tetragonal $BiVO_4$ has been interpreted as a consequence of a strong linear coupling between the TA and TO modes.[7,9] The isostructural compound $LaNbO_4$ exhibits a ferroelastic phase transition at $T_c = 528$ K.[1,4] For $LaNbO_4$ the corresponding TA mode shows the complete softening around T_c, whereas the TO mode with B_g symmetry is temperature independent.[10,11] In general, the acoustic symmetry axes on the (0,0,1) plane in scheelite-structure crystals do not coincide with the high-symmetry [1,0,0] and [1,1,0] directions.[12–14] Theoretical and experimental studies for $BiVO_4$ and $LaNbO_4$ showed that the soft TA modes exist along one of the acoustic symmetry axes.[6,7,10,15] However, previous investigations on phonon properties of the two compounds were limited in the vicinity of the Brillouin zone center. It is hoped that the phonon dispersion curves along the acoustic and crystallographic symmetry axes can provide useful information on the ferroelastic phase transition in $BiVO_4$. In this paper, we present an inelastic neutron scattering study of lattice dynamics of $BiVO_4$ in the paraelastic phase along the acoustic symmetry directions. The measured phonon dispersion curves and derived elastic constants are compared with results from Brillouin scattering measurements.[7] We also report an elastic central peak associated with the $[0.7\xi,\xi,0]$ TA mode and an elastic diffuse streak along $[1,\bar{1},0]$.

II. EXPERIMENT

Single crystals of $BiVO_4$ were grown by the floating-zone method, annealed in air at 1120 K for 6 h, and then cooled to room temperature. Cylindrical crystals were 7 mm in diameter and 25 mm in height, with the cylindrical axis parallel to the [0, 0,1] direction. The crystal was mounted in an aluminum holder and placed inside a furnace so that the [0, 0,1] crystal axis is perpendicular to the scattering plane. Neutron scattering measurements were performed using the T1-1 triple-axis spectrometer installed on the thermal guide of JRR-3M, Tokai, JAEA. Pyrolitic graphite (PG) crystals were used both as a monochromator and analyzer. The incident neutron energy was fixed at 14.7 meV for the T1-1 spectrometer. A PG filter was placed before the sample to suppress higher-order contamination. The collimation of 10′-10′-10′, 40′-10′-10′, or 40′-20′-20′ was set for experiments in the energy range lower than 1.5 meV, whereas the collimation of 40′-40′-40′ was used in the higher-energy range. The corresponding energy resolutions were 0.30, 0.39, 0.43, and 0.65 meV in full width at half maximum (FWHM) at zero energy transfer. Most measurements were performed at $T = 538$ K ($T_c + 10$ K), but the selected phonons were also studied up to $T = 873$ K ($T_c + 345$ K). Constant-**Q** scans were made around (2,2,0) with polarization in the (0,0,1) plane. The low-q phonon data were determined on the condition that the Bragg peak contamination is absent.

III. PHONON DISPERSION RELATIONS

A. Acoustic phonon symmetry

Generally, the $\langle 1,0,0\rangle$ and $\langle 1,1,0\rangle$ directions in scheelite crystals are different from the acoustic symmetry $\langle\gamma\rangle$ and

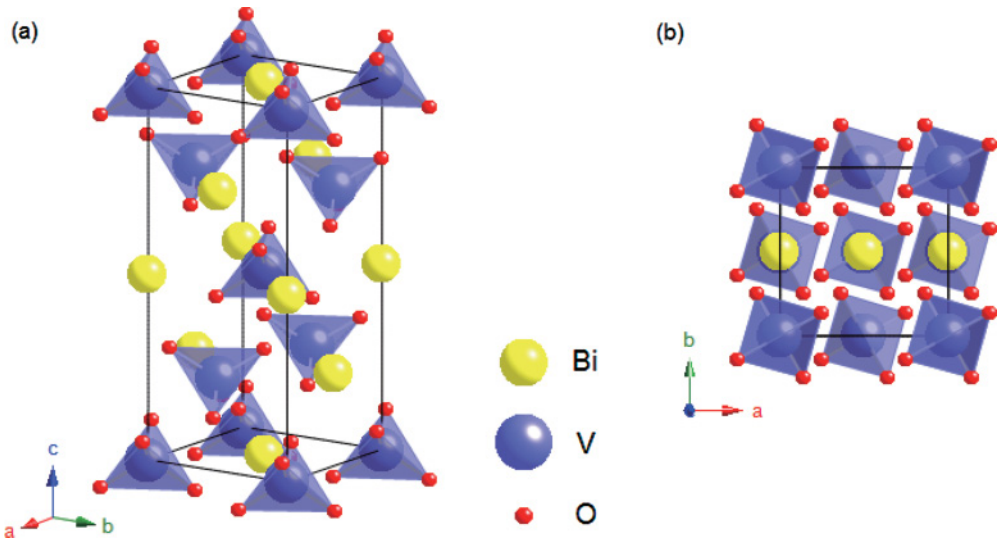

FIG. 1. (Color online) (a) Crystal structure of tetragonal $BiVO_4$. Atomic positions are taken from Ref. 5. (b) The projection of tetragonal $BiVO_4$ on the (0,0,1) plane.

$\langle\kappa\rangle$ axes.[12–14] The TA velocity on the (0,0,1) plane polarized on this plane shows the maximum along the $\langle\gamma\rangle$ direction, whereas the TA velocity reaches the maximum along the $\langle\kappa\rangle$ direction. The minimum TA velocity v_γ and the maximum TA velocity v_κ in the (0,0,1) plane are determined by[7,15]

$$\rho v_\gamma^2 = \tfrac{1}{4}(C_{11} - C_{12} + 2C_{66}) - \tfrac{1}{4}\left[(C_{11} - C_{12} - 2C_{66})^2 + 16C_{16}^2\right]^{1/2}, \quad (1)$$

$$\rho v_\kappa^2 = \tfrac{1}{4}(C_{11} - C_{12} + 2C_{66}) + \tfrac{1}{4}\left[(C_{11} - C_{12} - 2C_{66})^2 + 16C_{16}^2\right]^{1/2}, \quad (2)$$

where ρ is the density. For $BiVO_4$ and $LaNbO_4$, the soft acoustic mode along $\langle\gamma\rangle$ corresponds to the effective elastic constant $C_\gamma = \rho v_\gamma^2$, and the other mode along $\langle\kappa\rangle$ is connected with the effective elastic constant $C_\kappa = \rho v_\kappa^2$. The orientations of these axes from the [1,0,0] axis are given by the angle

$$\phi_A = \frac{1}{4}\arctan\left(\frac{4C_{16}}{C_{11} - C_{12} - 2C_{66}}\right), \quad (3)$$

where the suffix A refers to γ or κ.

The acoustic symmetry in scheelite crystals has been discussed in terms of the elastic constants. It is clearly necessary to distinguish between the acoustic and crystal symmetry axes in the entire Brillouin zone. In this study, we measured the angular dependence of the TA phonon energies polarized in the (0,0,1) plane at $\mathbf{q} = 0.141[\cos\theta, \sin\theta, 0]$, where the angle θ from the [1,0,0] direction in the (0,0,1) plane is varied between 0 and 90°. Figure 2 shows typical constant-$\mathbf{Q}$ scans at $\mathbf{Q} = (2 + 0.141\sin\theta, 2 - 0.141\cos\theta, 0)$ measured at $T = 773$ K ($T_c + 245$ K). Note that the phonon peak energy and its FWHM show the minimum at $\mathbf{q} = 0.141[\cos 55°, \sin 55°, 0]$, also expressed as $\mathbf{q} = 0.116[0.7, 1, 0]$. Thus the acoustic symmetry axis for the minimum phonon energy in $BiVO_4$ lies along the direction $\mathbf{q} = [0.7\xi, \xi, 0]$. The angle $\theta = 55°$ for the $[0.7\xi, \xi, 0]$ direction is in good agreement with the propagation angle ϕ_γ for v_γ determined by Brillouin scattering experiments.[7]

Figure 3 shows that the TA phonon dispersion curves along the $[0.7\xi, \xi, 0]$ and $[\xi, \xi, 0]$ directions measured at 773 K. The $[0.7\xi, \xi, 0]$ TA phonon curve in the range $\xi \geqslant 0.12$ is slightly lower than the $[\xi, \xi, 0]$ TA phonon curve. In particular, the energy difference between these modes becomes large with increasing ξ. Figures 2 and 3 indicate that the minimum TA phonon energy appears along the $[0.7\xi, \xi, 0]$ direction. It follows that the acoustic symmetry axis for the maximum phonon energy coincides with the $[\xi, 0.176\xi, 0]$ direction. An attempt to determine the $[\xi, 0, 0]$ TA phonon curve was unsuccessful, due to the extremely weak phonon intensities. Here we concentrated on the measurement of the TA mode along $[\xi, 0.176\xi, 0]$ direction. Figure 4 shows the TA phonon dispersion relations along $[\xi, 0.176\xi, 0]$ and $[0.7\xi, \xi, 0]$ measured at 538 K (T_c + 10 K). The energy of the $[0.7\xi, \xi, 0]$ TA phonon is higher than that of the $[\xi, 0.176\xi, 0]$ TA phonon at the same absolute value of $\mathbf{q}$. The anisotropic TA phonon dispersion curves in the limit $\xi \to 0$ are connected with the sound velocities given by Eqs. (1) and (2).

Ultrasonic and Brillouin scattering measurements of the sound velocities were carried out for the oxide scheelites $BiVO_4$, $LaNbO_4$, $CaMoO_4$, $SrMoO_4$, $PbMoO_4$, and $CaWO_4$.[7,10,12,13] These studies show the general tendency that the elastic constants C_{ij} in the (0,0,1) plane of AMO_4 are strongly related to the rotation of the isolated MO_4 (M = V, Nb, Mo, and W) tetrahedra. In $BiVO_4$, the V atom in VO_4 tetrahedra is tightly bonded to four oxygens, whereas the Bi atom is surrounded by the eight nearest-neighbor oxygen

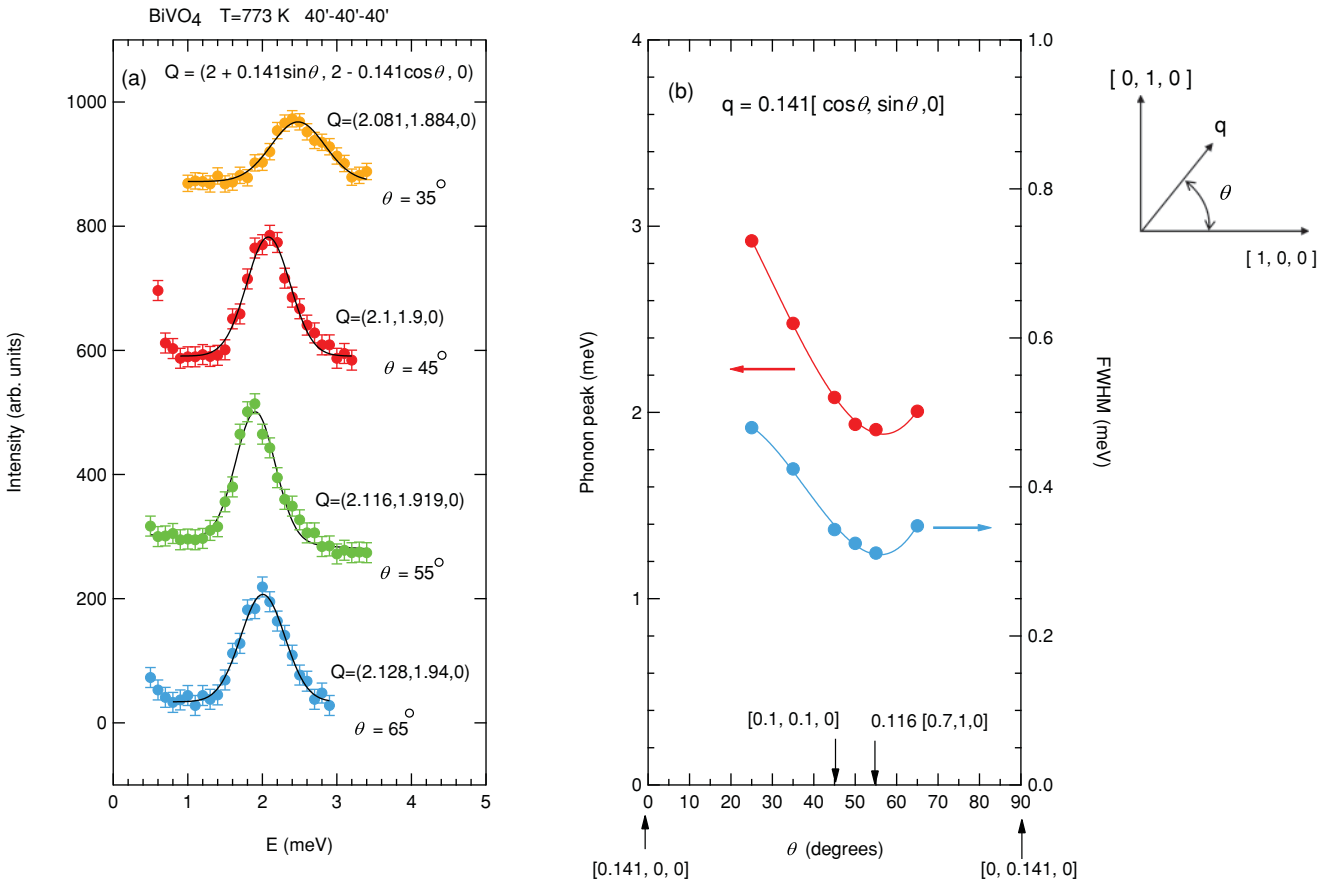

FIG. 2. (Color online) (a) Constant-**Q** scans for the TA phonons at $\mathbf{q} = 0.141[\cos\theta, \sin\theta, 0]$ polarized in the (0,0,1) plane in tetragonal $BiVO_4$. These data were taken at $T = 773$ K ($T_c + 245$ K). The solid lines are Gaussian fits to the data. (b) The angular dependence of TA phonon energy and its FWHM at $\mathbf{q} = 0.141[\cos\theta, \sin\theta, 0]$. The solid lines are drawn to guide the eye.

atoms. The V-O bond in the tetrahedra has a covalent character, and the Bi-O bond in BiO_8 is mainly ionic. The V-O bond length in VO_4 tetrahedra is 1.73 Å at 573 K and the Bi-O bonds in BiO_8 dodecahedra have slightly different lengths, 2.45 and 2.50 Å.[5] Thus we expect that the force constant between Bi and O atoms is considerably weaker than that for V and O atoms. The Bi atomic mass is 1.82 times as large as the tetrahedral mass of VO_4. Thus it is reasonable to expect that the Bi atom motion contributes significantly to the TA branches. The oxygen configuration in BiO_8 dodecahedra should determine the angular dependence of the interaction between Bi and O atoms on the (0,0,1) plane. Similarly, four oxygens in VO_4 tetrahedra have influence on the V atom motion in the (0,0,1) plane. It has been assumed that the MO_4 tetradedra in AMO_4 behave as the rigid units in the low-frequency lattice modes.[16–18] In this approximation, the TA modes of AMO_4 are described by the motion of the A atom and the rigid MO_4 unit, and the symmetry at four oxygens is not taken into account. However, the electronic structure calculations along the c axis of the scheelite oxides show a general feature that the electron charge distribution of MO_4 is not spherical.[19–22] Furthermore, the symmetry axis of the electronic charge density of $AgReO_4$ and $NaReO_4$ on the (0,0,1) plane is found to deviate from the crystal symmetry axis.[21] The motion of the rigid VO_4 is also sensitive to the nonspherical charge distribution around the V site. Consequently, the lower $[0.7\xi,\xi,0]$ TA branch in Fig. 3 is closely related to the fact that the oxygens in the scheelite structure occupy the lowest-symmetry positions.

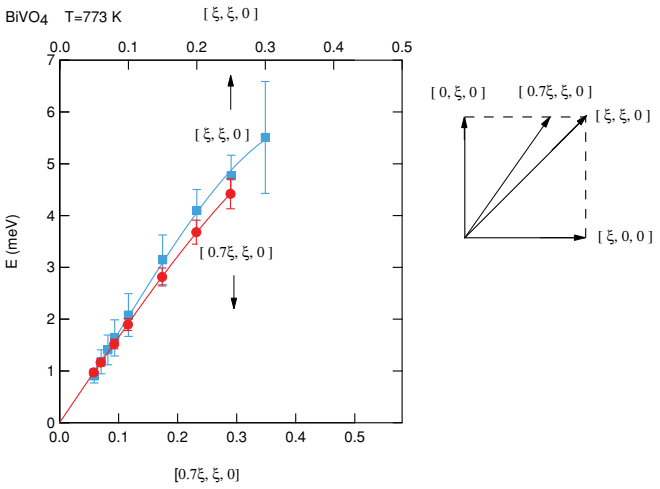

FIG. 3. (Color online) TA phonon dispersion curves along the $[\xi,\xi,0]$ and $[0.7\xi,\xi,0]$ directions in tetragonal $BiVO_4$. The data were taken at $T = 773$ K ($T_c + 245$ K). Each filled symbol and the attached bar refer to the phonon peak and its FWHM, respectively. The error bars for phonon peaks are smaller than the symbol size and are therefore omitted. The solid lines are guides to the eye.

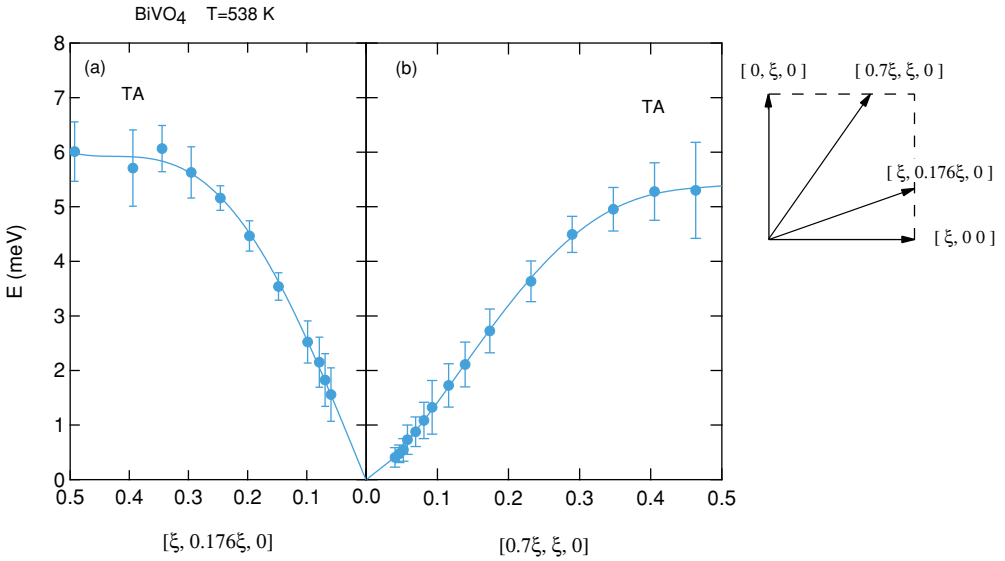

FIG. 4. (Color online) The TA phonon dispersion curves in tetragonal $BiVO_4$ along the [ξ,0.176ξ,0] and [0.7ξ,ξ,0] directions measured at 538 K. The polarization direction lies in the (0,0,1) plane. Each solid circle and the attached bar refer to the phonon peak and its FWHM, respectively. The lines are guides to the eye.

B. Temperature dependence of TA modes

Figure 5 shows that the temperature dependence of the [ξ,0.176ξ,0] TA and [0.7ξ,ξ,0] TA branches. Typical constant-**Q** scans at $q = [0.7\xi,\xi,0]$ will be shown in Sec. III C. The [ξ,0.176ξ,0] TA branch exhibits a hardening with decreasing temperature from 873 to 538 K ($T_c + 10$ K). This tendency is the normal behavior in an anharmonic lattice.[23] In contrast, the [0.7ξ,ξ,0] TA branch has quite different temperature dependence. The [0.7ξ,ξ,0] TA branch is weakly temperature dependent from 773 to 673 K, and then shifts downward with decreasing temperature to 538 K ($T_c + 10$ K) in the range $\xi \lesssim 0.2$. The [0.7ξ,ξ,0] TA branch in the range $\xi \gtrsim 0.2$ is almost temperature independent between 538 and 773 K. As shown in Fig. 5(b), the [0.7ξ,ξ,0] TA branch at 538 K has a slight upward curvature in the range $\xi \lesssim 0.1$.

Figure 6 shows the effective elastic constants C_κ and C_γ determined from the initial slopes of the [ξ,0.176ξ,0] and

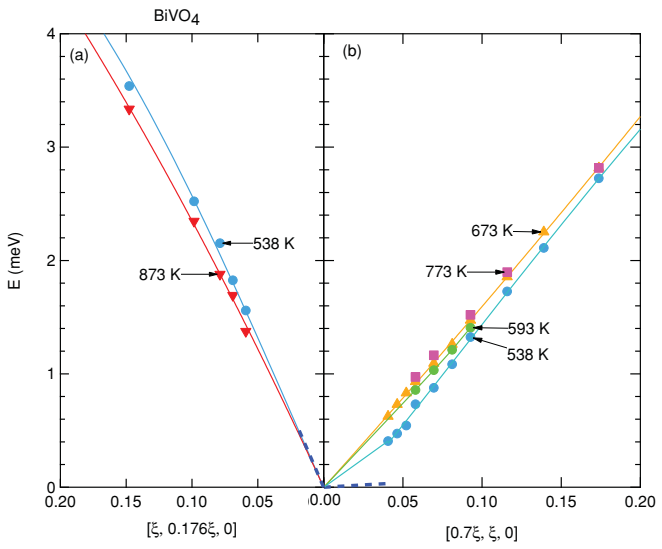

FIG. 5. (Color online) Temperature dependence of the [ξ,0.176ξ,0] TA and [0.7ξ,ξ,0] TA branches in $BiVO_4$. The filled symbols denote the phonon peak. The error bars are smaller than the symbol size. The solid lines are guides to the eye. The dashed lines around $\xi = 0$ represent the extrapolations of the sound velocities at $T = 527$ K determined by Brillouin scattering experiments (Ref. 7).

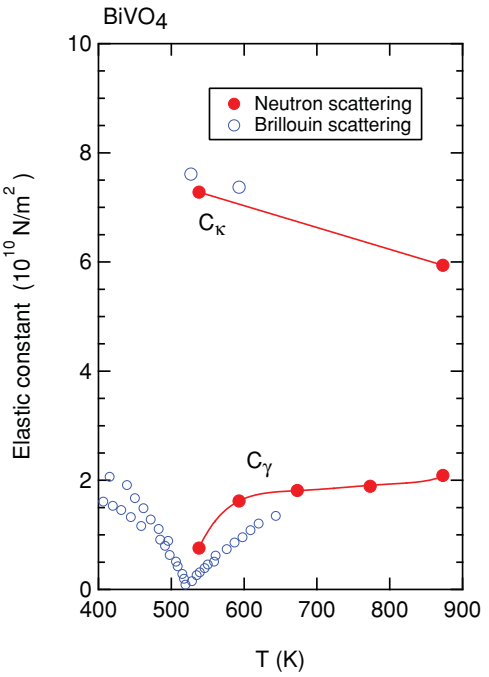

FIG. 6. (Color online) Effective elastic constants C_γ and C_κ for $BiVO_4$ as a function of temperature. Elastic constants derived from the inelastic neutron scattering data are compared with the Brillouin scattering data taken from Ref. 7. The lines are guides to the eye.

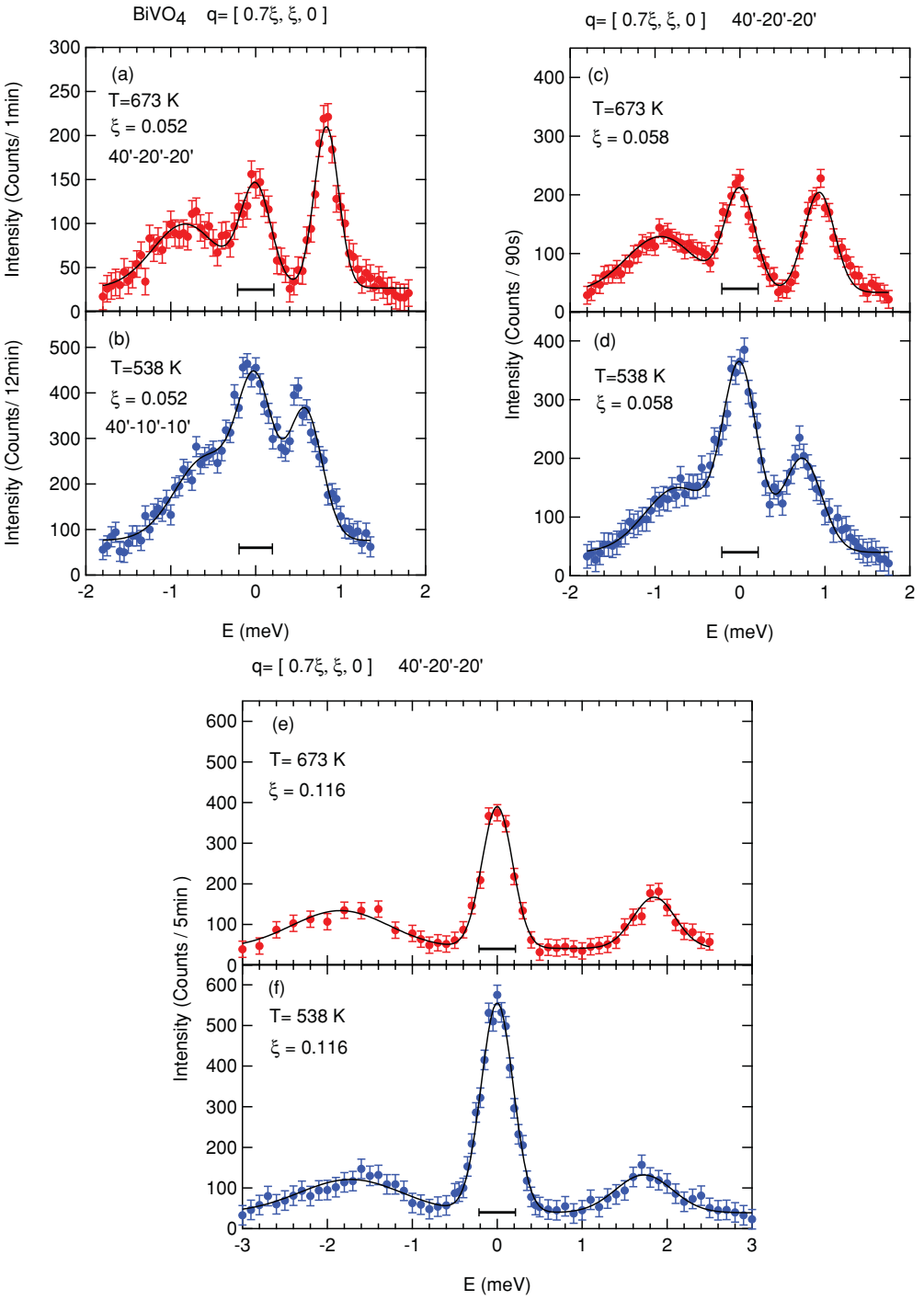

FIG. 7. (Color online) Constant-**Q** scans at $q = [0.7\xi,\xi,0]$ in $BiVO_4$ measured at $T = 538$ K (lower panels) and 673 K (upper panels). The solid lines are Gaussian fits to the data. The horizontal bars show the instrumental energy resolution.

$[0.7\xi,\xi,0]$ TA branches, respectively. The present results are compared with the Brillouin scattering data.[7] Good agreement between the two methods is obtained for the stiffened elastic constant C_κ near T_c. This indicates that the slope of the $[\xi,0.176\xi,0]$ TA branch is q independent up to 1.5 meV. In contrast, the moderate softening of C_γ toward T_c observed in this study is different from the complete softening determined by Brillouin scattering.[7] In this study the accessible lowest-energy peak is 0.4 meV at 538 K, whereas the energy of the soft TA mode observed by the Brillouin scattering is 8.3×10^{-3} meV at T_c.[7] A plausible explanation for the discrepancy in C_γ is that the complete softening of this TA mode occurs in the long wavelength limit.

The cubic to tetragonal transition in Nb_3Sn at $T_M = 45$ K has been considered as a typical example of ferroelastic phase transitions.[24–26] Inelastic neutron scattering showed the pronounced softening of the $[\xi,\xi,0]$ TA branch with displacement along $[1,\bar{1},0]$ in the entire ξ range as the

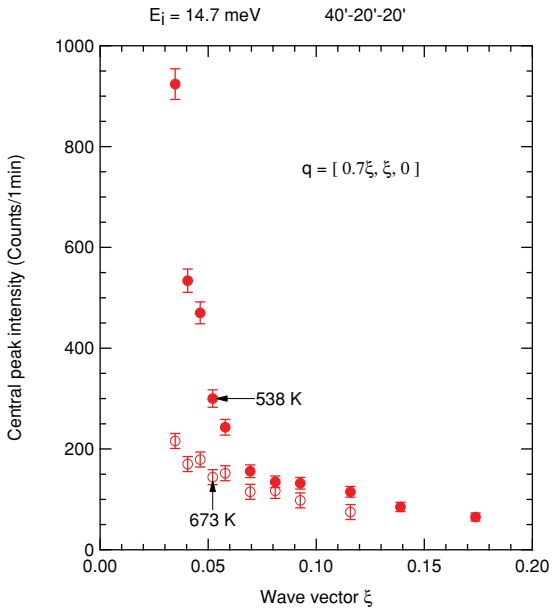

FIG. 8. (Color online) Central-peak intensities along the $[0.7\xi,\xi,0]$ direction measured at 538 and 673 K.

transition temperature is approached from above.[27,28] The elastic constant $C_e = \frac{1}{2}(C_{11} - C_{12})$ estimated from the initial slope of the $[\xi,\xi,0]$ TA branch at T_M is much higher than the value determined by ultrasonic measurements.[29] A similar discrepancy suggests that the soft TA branch has an upward curvature in the vicinity of $q = 0$ at the ferroelastic phase transition. Actually, the nonlinear TA dispersion curves associated with C_e were observed around the zone center for $Fe_{1-x}Pd_x$,[30] $In_{1-x}Tl_x$,[31,32] NbRu,[33] and $PrAlO_3$.[34,35] For a cubic-tetragonal transformed material, Barsh and Krumhansl[36] proposed a phenomenological model including strain and strain-gradient components. In their model, the upward TA phonon dispersion at small q is closely related to the premartensitic structure above T_M. The nonlinear TA phonon dispersion at low q in $BiVO_4$ may be explained on the basis of a similar free energy analysis for the tetragonal to monoclinic transition.

Raman scattering experiments[8,9] found a softening of the B_g TO mode along the [0,0,1] axis in tetragonal $BiVO_4$. The energies of the zone-center soft TO mode are 5.5 meV at 750 K and 3.9 meV at $T_c = 528$ K. The square of the soft TO mode energy extrapolates to zero at $T_0 = 365$ K.[8,9] On the basis of the Landau free-energy analysis, Pinczuk *et al.*[8,9] have interpreted the large difference $(T_c - T_0) = 163$ K as a consequence of the strong linear coupling between the lattice strain and the soft TO mode. Although $BiVO_4$ exhibits no piezoelectricity, the tetragonal S_4 symmetry at the Bi and V sites has been considered as the origin of the linear coupling

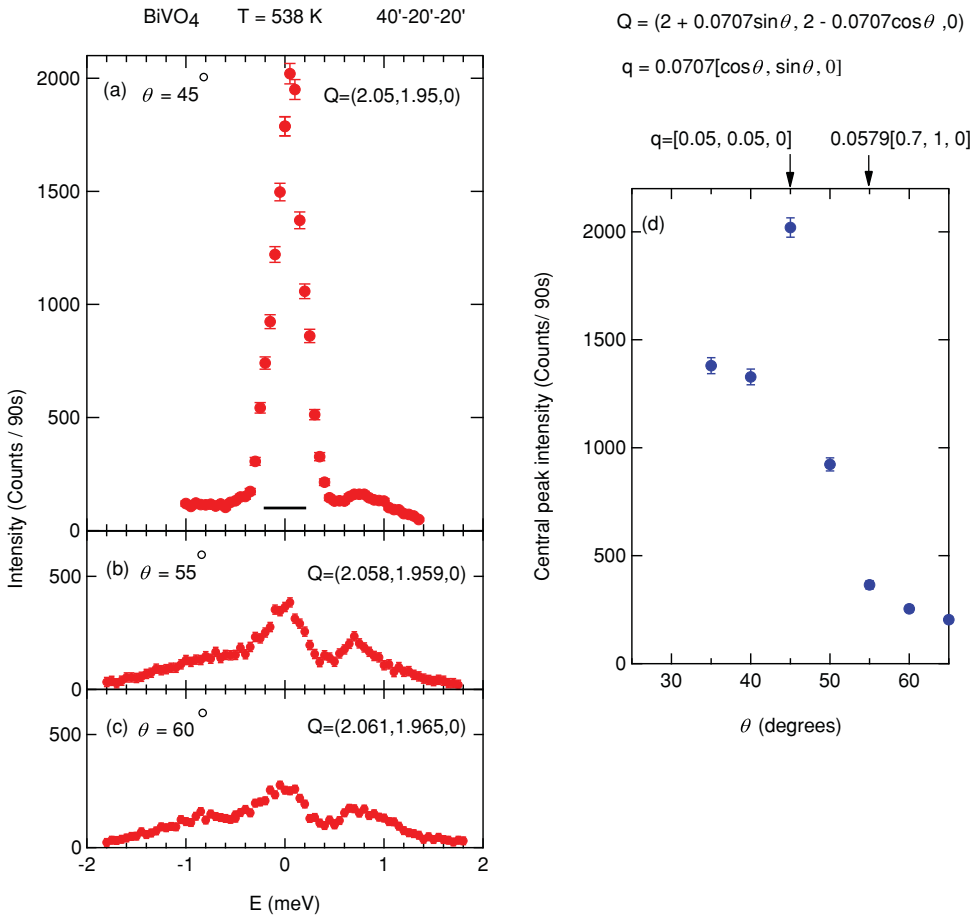

FIG. 9. (Color online) The angular dependence of constant-**Q** scans at $(2 + 0.0707 \sin\theta, 2 - 0.0707 \cos\theta, 0)$ measured at 538 K.

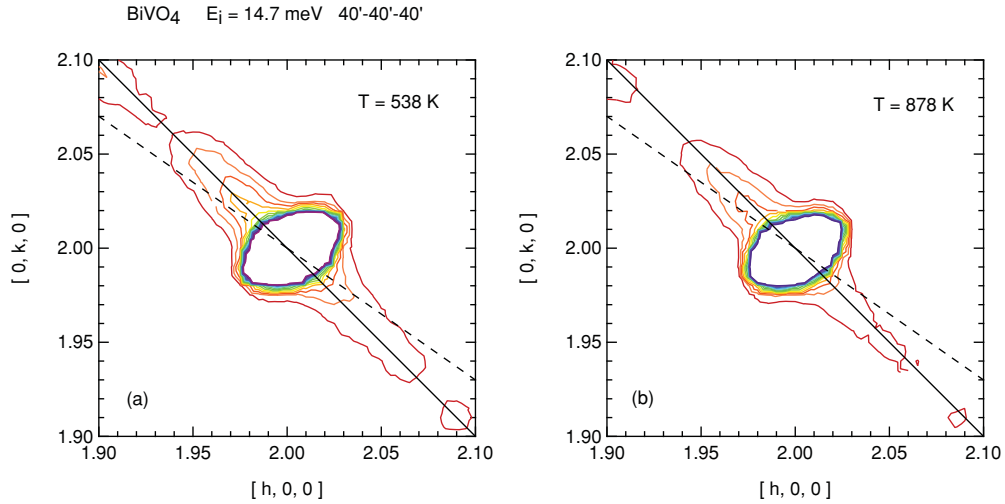

FIG. 10. (Color online) Contour maps of the elastic diffuse scattering around the (2,2,0) Bragg peak measured at (a) $T = 538$ K and (b) 878 K. For simplicity, we plot the data less than 4% of the Bragg peak at 538 K. Solid lines indicate the $[1,\bar{1},0]$ direction. Dashed lines indicate the direction along which the TA phonon dispersion shows the minimum energy.

effect.[7,9] As shown in Fig. 5, the significant softening of the $[0.7\xi,\xi,0]$ TA branch is confined to the low-q region. The $[0.7\xi,\xi,0]$ TA branch behaves normally except for the low-q region. In addition, the energy of the soft TA mode is much lower than that for the soft TO mode. Thus the present study found no evidence of the strong linear coupling with the TO mode. For the related compound $LaNbO_4$ Brillouin scattering measurements revealed the complete softening of the TA mode at $T_c = 528$ K, whereas Raman scattering experiments found that the energy of the B_g TO mode remains at 11 meV.[10,11] These studies indicate the absence of the linear coupling in the ferroelastic phase transition of $LaNbO_4$.

C. Central peak

Figure 7 shows typical constant-**Q** scans along $q = [0.7\xi,\xi,0]$ measured at $T = 538$ K ($T_c + 10$ K) and 673 K. A pair of the TA phonon modes indicates the softening as the temperature approaches T_c. Moreover, an elastic central peak grows around $E = 0$. The FWHM of the central peak is comparable to the instrumental resolution. We determined the central-peak intensities along $[0.7\xi,\xi,0]$. Figure 8 shows that the central-peak intensity increases with decreasing temperature toward T_c. Next we measured the angular dependence of the central peak. Constant-**Q** scans in Fig. 9 show that the central peak intensity for $q = [\xi,\xi,0]$ is significantly higher than that for $q = [0.7\xi,\xi,0]$.

For comparison, we performed elastic neutron scattering measurements around the (2,2,0) reflection. Figure 10 shows that the elastic diffuse streak along $[1,\bar{1},0]$ remains up to 838 K. Thus the diffuse streak should enhance the central peak associated with the $[\xi,\xi,0]$ TA mode. It has been pointed out that the propagating direction of the soft TA mode in tetragonal $BiVO_4$ corresponds to the orientation of domain walls below T_c.[6,37] This scenario predicts that the soft TA mode gives rise to the elastic diffuse streak along the $[0.7\xi,\xi,0]$ direction above T_c. However, the present results in Fig. 10 do not support the prediction. The diffuse streak along $[1,\bar{1},0]$ may be related with the randomly distributed defects or the lattice distortion above T_c. One possibility is that the crystal symmetry above T_c constrains the distribution of the elastic diffuse streak related with the soft TA mode. Another possibility is that the central peak associated with the $[0.7\xi,\xi,0]$ TA mode has a dynamical origin. In this case, the central peak corresponding to the $[0.7\xi,\xi,0]$ TA mode is mainly independent of the presence of the diffuse streak along $[1,\bar{1},0]$. The central peak associated with the softening of the TA mode around $q = 0$ has been observed in Nb_3Sn,[27,28] $PrAlO_3$,[34,35] $TbVO_4$,[38] and $(KBr)_{(1-x)}(KCN)_x$.[39] In the cubic to tetragonal martensitic transition, the softening of the $[\xi,\xi,0]$ TA branch related with C_e has been discussed in connection with the precursor tweed structure and the diffuse streak along $[1,\bar{1},0]$.[40–43] The relation among the diffuse streak, the central peak, and the soft mode may be more complicated in $BiVO_4$, in view of the distinction between acoustic and crystal symmetry. Further studies of the precursor structure in $BiVO_4$ are needed to clarify the interplay between the TA phonon softening and the central peak.

IV. CONCLUSION

The TA phonon-dispersion relations for tetragonal $BiVO_4$ show that the acoustic symmetry axis on the (0,0,1) plane deviates from the high-symmetry axis $[\xi,\xi,0]$. The distinction between the acoustic and crystallographic symmetry axes comes from the scheelite structure in which the VO_4 tetrahedra are rotated about the [0, 0,1] axis. The $[0.7\xi,\xi,0]$ TA branch softens slightly $\xi \lesssim 0.2$ as the temperature approaches T_c from above. We estimated the effective elastic constant C_γ from the initial slope of the $[0.7\xi,\xi,0]$ TA branch. The observed softening of C_γ is quite different from the complete softening of the TA mode reported from Brillouin scattering measurements. These results suggest that the complete softening of this TA

mode occurs in the long-wavelength limit. The softening of the $[0.7\xi,\xi,0]$ TA mode gives rise to the narrow central peak. Furthermore, the elastic diffuse streak along $[1,\bar{1},0]$ remains up to 878 K. The coexistence of the central peak and the diffuse streak is discussed in connection with the softening of the $[0.7\xi,\xi,0]$ TA mode.

ACKNOWLEDGMENTS

We are grateful to Satoshi Iida, Masahiko Hayashi, and Hiromi Unoki for valuable discussions. We also thank Yasuaki Oohara for technical support during the neutron scattering experiment.

*tomeno@gipc.akita-u.ac.jp

[1] J. D. Bierlein and A. W. Sleight, Solid State Commun. **16**, 69 (1975).
[2] L. Hoffart, U. Heider, R. A. Huggins, W. Witschel, R. Jooss, and A. Lentz, Ionics **2**, 34 (1996).
[3] A. Kudo, K. Omori, and H. Kato, J. Am. Chem. Soc. **121**, 11459 (1999).
[4] W. I. F. David and I. G. Wood, J. Phys. C **16**, 5127 (1983).
[5] W. I. F. David, A. M. Glazer, and A. W. Hewat, Phase Transitions **1**, 155 (1979).
[6] G. Benyuan, M. Copic, and H. Z. Cummins, Phys. Rev. B **24**, 4098 (1981).
[7] H. Tokumoto and H. Unoki, Phys. Rev. B **27**, 3748 (1983).
[8] A. Pinczuk, G. Burns, and F. H. Docal, Solid State Commun. **24**, 163 (1977).
[9] A. Pinczuk, B. Welber, and F. H. Docal, Solid State Commun. **29**, 515 (1979).
[10] K. Hara, A. Sakai, S. Tsunekawa, A. Sawada, Y. Ishibashi, and T. Yagi, J. Phys. Soc. Jpn. **54**, 1168 (1985).
[11] M. Wada, Y. Nakayama, A. Sawada, S. Tsunekawa, and Y. Ishibashi, J. Phys. Soc. Jpn. **47**, 1575 (1979).
[12] J. M. Farley and G. A. Saunders, J. Phys. C **5**, 3021 (1973).
[13] J. M. Farley, G. A. Saunders, and D. Y. Chung, J. Phys. C **8**, 780 (1975).
[14] P. Blanchfield and G. A. Saunders, J. Phys. C **12**, 4673 (1979).
[15] W. I. F. David, J. Phys. C **16**, 5119 (1983).
[16] S. P. S. Porto and J. F. Scott, Phys. Rev. **157**, 716 (1967).
[17] G. Venkataraman and V. C. Sahni, Rev. Mod. Phys. **42**, 409 (1970).
[18] H. Kanamori, S. Hayashi, and Y. Ikeda, J. Phys. Soc. Jpn. **36**, 511 (1974).
[19] Y. Zhang, N. A. W. Holzwarth, and R. T. Williams, Phys. Rev. B **57**, 12738 (1998).
[20] Y. Abraham, N. A. W. Holzwarth, and R. T. Williams, Phys. Rev. B **62**, 1733 (2000).
[21] J. Spitaler, C. Ambrosch-Draxl, E. Nachbaur, F. Belaj, H. Gomm, and F. Netzer, Phys. Rev. B **67**, 115127 (2003).
[22] A. Walsh, Y. Yan, M. N. Huda, M. M. Al Jassim, and S.-H. Wei, Chem. Mater. **21**, 547 (2009).
[23] G. Leibfried and W. Ludwig, in *Advances in Research and Applications*, Solid State Physics, Vol. 12, edited by F. Seitz and D. Turnbull (Academic, New York, 1961), pp. 275–444.
[24] R. A. Cowley, Phys. Rev. B **13**, 4877 (1976).
[25] E. K. H. Salje, *Phase Transitions in Ferroelastic and Co-elastic Crystals* (Cambridge University Press, Cambridge, England, 1990).
[26] B. Lüthi, *Physical Acoustics in the Solid State* (Springer-Verlag, Berlin, 2005).
[27] G. Shirane and J. D. Axe, Phys. Rev. Lett. **27**, 1803 (1971).
[28] J. D. Axe and G. Shirane, Phys. Rev. B **8**, 1965 (1973).
[29] W. Rehwald, M. Rayl, R. W. Cohen, and G. D. Cody, Phys. Rev. B **6**, 363 (1972).
[30] M. Sato, B. H. Grier, S. M. Shapiro, and H. Miyajima, J. Phys. F **12**, 2117 (1982).
[31] T. R. Finlayson, M. Mostoller, W. Reichardt, and H. G. Smith, Solid State Commun. **53**, 461 (1985).
[32] T. Finlayson and H. Smith, Metall. Mater. Trans. A **19**, 193 (1988).
[33] S. M. Shapiro, G. Xu, G. Gu, J. Gardner, and R. W. Fonda, Phys. Rev. B **73**, 214114 (2006).
[34] J. K. Kjems, G. Shirane, R. J. Birgeneau, and L. G. Van Uitert, Phys. Rev. Lett. **31**, 1300 (1973).
[35] R. J. Birgeneau, J. K. Kjems, G. Shirane, and L. G. Van Uitert, Phys. Rev. B **10**, 2512 (1974).
[36] G. R. Barsch and J. A. Krumhansl, Phys. Rev. Lett. **53**, 1069 (1984).
[37] W. I. F. David, J. Phys. C **16**, 5093 (1983).
[38] M. T. Hutchings, R. Scherm, S. H. Smith, and S. R. P. Smith, J. Phys. C **8**, L393 (1975).
[39] K. Knorr, A. Loidl, and J. K. Kjems, Phys. Rev. Lett. **55**, 2445 (1985).
[40] S. M. Shapiro, B. X. Yang, Y. Noda, L. E. Tanner, and D. Schryvers, Phys. Rev. B **44**, 9301 (1991).
[41] S. Kartha, T. Castán, J. A. Krumhansl, and J. P. Sethna, Phys. Rev. Lett. **67**, 3630 (1991).
[42] C. S. Becquart, P. C. Clapp, and J. A. Rifkin, Phys. Rev. B **48**, 6 (1993).
[43] S. Kartha, J. A. Krumhansl, J. P. Sethna, and L. K. Wickham, Phys. Rev. B **52**, 803 (1995).